Integrating longitudinal imaging and transcriptomics in single cells using CellCage™ Technology reveals cellular heterogeneity beyond gene expression

Pier Federico Gherardini[1], Mehdi Mohseni[1], Shreya S. Deshmukh[1], Shan Sabri[1], Richard Yau[1], Yining Chen[2], Makenzie Sacca[1], Nirvan Rouzbeh[1], Olaia Villa[1], Gaetano Viscido[2], James Walker[3], Joseph Ecker[3], Andrea Califano[2]

[1]Cellanome, Foster City, CA, [2]CZ Biohub New York, New York, NY, [3]Salk Institute for Biological Sciences, Department of Plant Biology, La Jolla, CA, USA

The relationship between gene expression and cellular function is complex: transcriptomic measurements provide static snapshots, while cellular phenotypes unfold over time. To bridge this gap, we developed CellCage™ Technology, which leverages light-guided hydrogel polymerization to enable longitudinal imaging of individual cells coupled with endpoint transcriptomics. Within this system, imaging provides unambiguous readouts of complex cellular functions linked to underlying transcriptional programs. To characterize information-rich imaging phenotypes, we leveraged DINOv2, a self-supervised vision transformer, to extract high-dimensional morphological features with dimensionality comparable to gene expression. This combination of imaging and transcriptomics represents a novel paired datatype that reveals biological insights inaccessible to transcriptomics alone. In drug-treated lung cancer cells, longitudinal monitoring identified a stochastic, non-mutational resistant state associated with potassium channel overexpression and p53-mediated quiescence. In preadipocytes and microglia, paired data uncovered functional driver genes that transcriptomic clustering alone failed to identify

Cellanome R3200: A Platform Integrating Longitudinal Live Cell Imaging With Transcriptomics

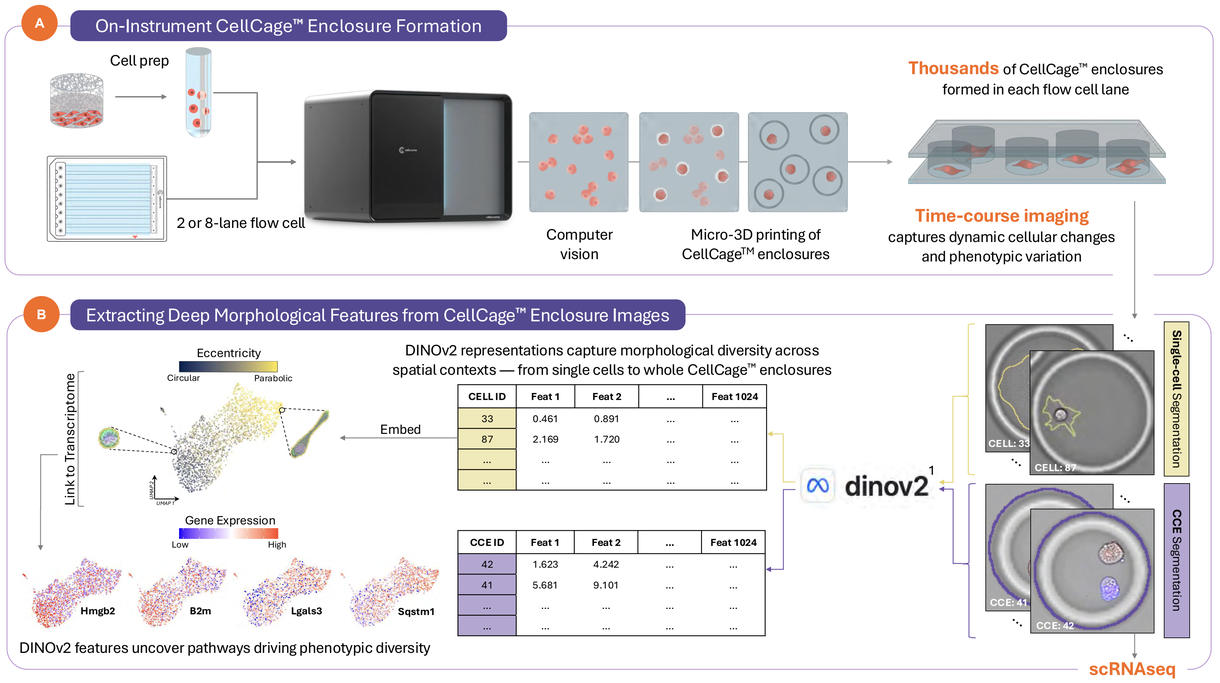

Fig. 1. Integrated experimental and computational workflow linking morphology and transcriptomics. A: Schematic of Cellanome's CellCage™ technology, which enables multi-modal phenotypic and functional profiling of the same live cells. Tens of thousands of cells are mixed with a hydrogel precursor and loaded into a multi-lane flow cell. Individual cells are located, and CellCage™ enclosures (CCEs) are automatically generated around them via light-guided polymerization. The CCEs are permeable to small molecules and antibodies, allowing long-term culture and time-course imaging of the same cells. Following imaging-based assays, cells are lysed *in situ*, and mRNA is captured for cDNA synthesis, library preparation, and sequencing on an external instrument. **B:** DINOv2-based computational workflow for extracting high-dimensional morphological embeddings from CCE images. These features capture phenotypic variation across scales — from single cells to entire CCEs — and can be integrated with single-cell transcriptomic data to reveal morphology–gene expression relationships.

DINOv2: A Self-Supervised Model for Extracting Morphological Features from Images

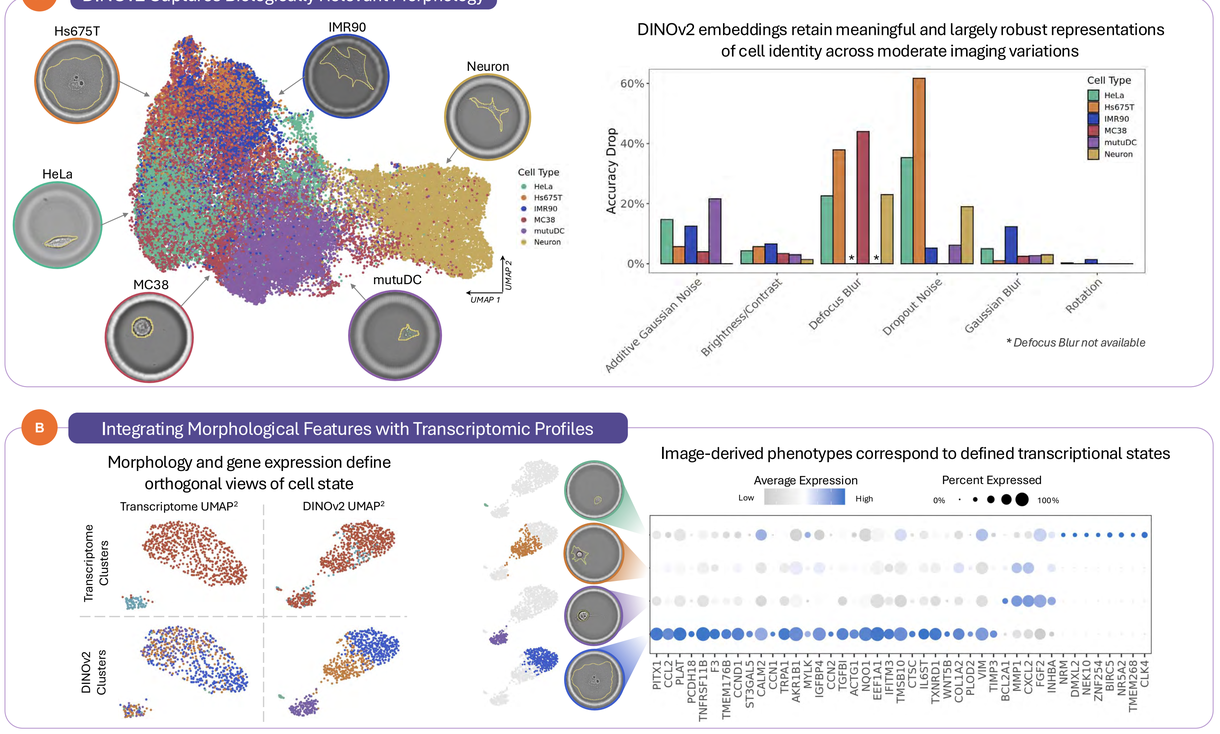

Fig. 2. Validation of DINOv2 morphological embeddings. A: DINOv2 features from six cell lines clustered by cell identity, confirming capture of meaningful morphological differences. Embedding similarity predicted the generalization performance of a Mask R-CNN (Region-based Convolutional Neural Network) segmentation model. The embeddings remained robust under common image augmentations, supporting their use for integration with transcriptomic data. **B:** Clustering of DINOv2 features from fibroblast CCE images identified four distinct morphological states — ranging from fully adhered, ECM-enriched cells (CCN2, ST3GAL5; Blue cluster) to weakly adhered, inflammatory cells (CXCL2, MMP1; Orange cluster), with intermediate adhesion–stress profiles. These morphology-defined phenotypes were undetectable by transcriptomic clustering alone, demonstrating that image-derived embeddings capture functionally relevant cellular heterogeneity.

Longitudinal Imaging Combined With Transcriptomics Identifies Drug Resistant States

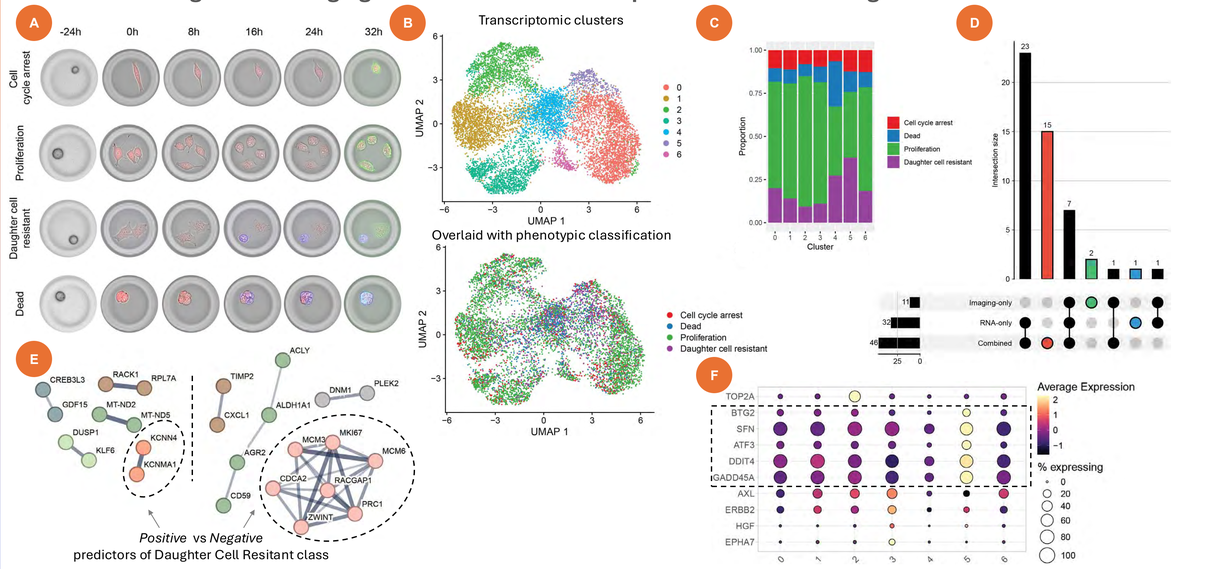

Fig. 3. Response of A549 lung cancer cells to treatment with Olmutinib, an EGFR inhibitor. A: A549 cells were treated with 10 μM Olmutinib and imaged over 32 hours. CCEs were classified in different phenotypes based on the analysis of longitudinal imaging data. **B**: UMAP visualization and unsupervised clustering of the transcriptomic data (top), colored by the phenotypic classification (bottom). **C**: each transcriptomic cluster contains cells spanning all four of the imaging-based phenotypes, revealing limited concordance between the two classification types. **D**: Upset plot showing overlap of significant GSEA pathway enrichments across three classification strategies. The combination of transcriptomic clustering with imaging classification identified 15 unique pathways not found in either single-modality strategy. **E**: Gene networks that are positive (left) or negative (right) predictors of the Daughter Cell Resistant class. Positive predictors include Ca-activated K channels, negative predictors comprise cell cycle genes. **F**: The Daughter Cell Resistant class is over-represented in cluster 5 (panel C), which includes p53 transcriptional targets associated with a quiescent/slow-cycling drug resistant state

Longitudinal Imaging Combined With Transcriptomics Identifies Drivers of Preadipocytes Differentiation

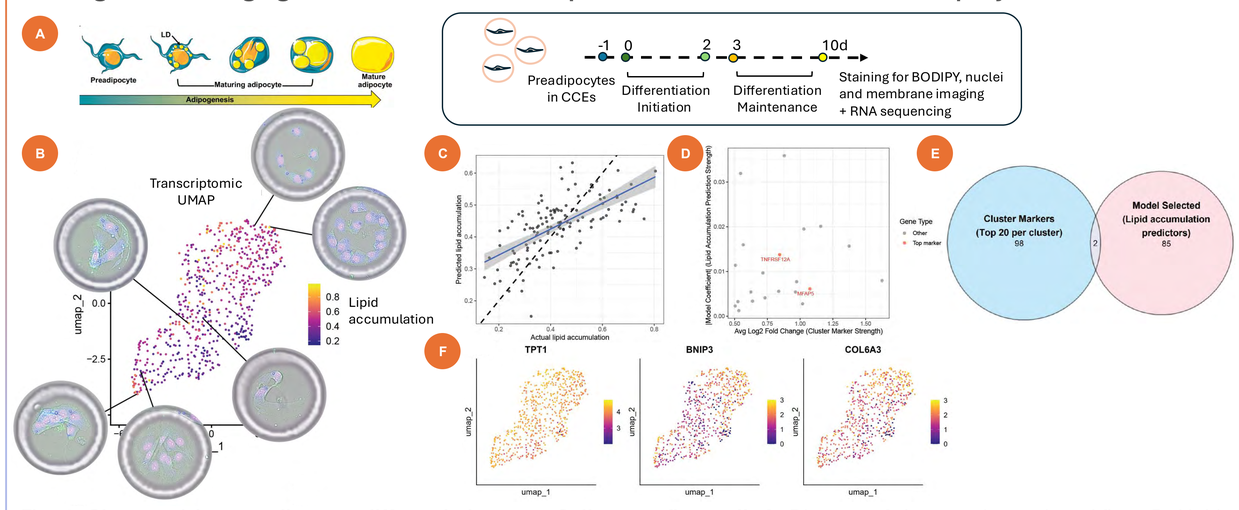

Fig. 4. Characterizing preadipocyte differentiation on a Cellanome flow cell. A: Diagram of the experimental workflow. **B**: Lipid accumulation score (ratio of BODIPY to nuclear signal) does not segregate with global transcriptomic patterns. **C**: ElasticNet prediction of lipid accumulation scores from gene expression data. The x and y axis correspond to the actual and predicted values respectively. **D**: Average Log2 fold-change between clusters (x axis) vs absolute model coefficient (y axis) for the genes selected by the model. Red genes are among the top-20 differentially expressed genes between transcriptomic clusters. **E**: Overlap between top-20 differentially expressed genes between transcriptomic clusters (blue) and model-selected predictors of lipid accumulation (pink). **F**: Expression UMAP colored by the top-3 positive model predictors, showing that the expression values of these genes are uniformly distributed

A Functional Assay To Identify Genes Associated With Phagocytic Activity

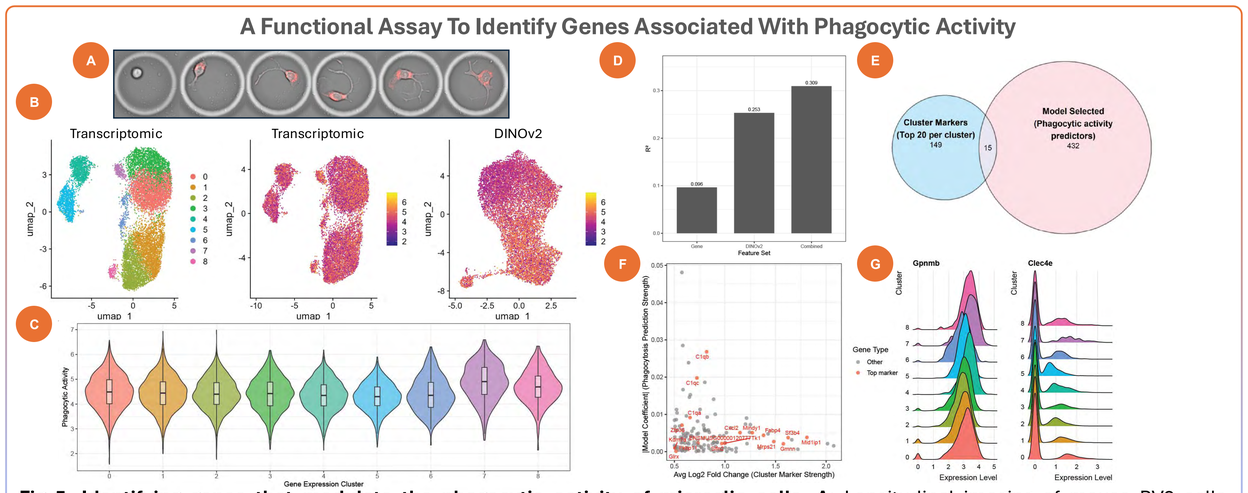

Fig 5. Identifying genes that modulate the phagocytic activity of microglia cells. A: Longitudinal imaging of mouse BV2 cells phagocytosing pHrodo particles. **B**: UMAPs based on the gene expression data (left and center), show that phagocytic activity is uniformly distributed. The UMAP based on the DINOv2 features (right) shows better correlation. **C**: Distribution of phagocytic activity across expression-derived clusters. **D**: R^2 performance of different ElasticNet models trained to predict phagocytic activity. **E**: Minimal overlap between top-20 differentially expressed genes between transcriptomic clusters and model-selected predictors of phagocytic activity. **F**: Average Log2 fold-change between clusters (x axis) vs absolute model coefficients (y axis) for the genes selected by the expression-only model. Red genes are among the top-20 differentially expressed genes between transcriptomic clusters. **G**: Gpnmb and Clec4e are among the top positive predictors for the gene expression-based model and have clear mechanistic evidence linking them to the phagocytosis process. However, their expression is very similar across all the transcriptomic clusters.